

ALLOTROPIC TRANSFORMATION OF COBALT IN MAGNETIC INDUCTION MELTED $\text{Fe}_{60}\text{Al}_{1-x}\text{Co}_x$

Abdelhak Fekrache¹⁾, Mohamed Yacine Debili^{1)*}, Halima Boularas¹⁾, Douniazed Lamrous¹⁾, Nacira Sassane¹⁾

¹⁾ LM2S, Physics department, Faculty of science, Badji-Mokhtar-Annaba University, Algeria

Received: 13.05.2013

Accepted: 22.10.2013

*Corresponding author: e-mail: mydebili@yahoo.fr, Tel.: +213 38872770, LM2S, Physics department, Faculty of science, Badji-Mokhtar-Annaba University 23200 Annaba, Algeria

Abstract

In contrast to the abundance of studies in Fe-Al and Fe-Co, those in the Fe-Al-Co ternary system are scarce. Consequently, the phase separation and phase diagram of this system remain still ambiguous. Ternary $\text{Fe}_{0.6}\text{Al}_{1-x}\text{Co}_x$ (x values in a molar ratio of 0.05, 0.1, 0.15, and 0.2) have been elaborated by high frequency magnetic induction fusion, in order to study the effect of cobalt ternary addition on the structural behavior such as phase separation, thermal and mechanical properties of Fe-based alloy system, by means of x-ray diffraction, thermal analysis (DSC) and Vickers microhardness. An unexpected allotropic phase transformation from stable HCP to metastable FCC Cobalt has been observed in all alloys.

Keywords: Fe-Al-Co, phase transformation, phase separation, lattice parameter

1 Introduction

Numerous technological applications require the use of intermetallic alloys. New materials can be made relatively easily by changing the stoichiometry of the intermetallic alloys and their crystal structures. Of particular interest are the transition metal aluminides, e.g. FeAl, NiAl, and CoAl, which are resistant to corrosion and oxidation, have interesting magnetic properties [1], and are used as high-temperature structural materials and soft magnetic materials. The binary $\text{Al}_{13}\text{Fe}_4$ and $\text{Al}_{13}\text{Co}_4$ compounds form polytetrahedral phases closely related to quasicrystals. $\text{Al}_{13}\text{Fe}_4$ is a monoclinic approximant phase [2]. Cobalt is usually added to the alloys to improve their cycling stability and discharge capacity [3–4]. There are some works done on low-Co alloys in which Co was substituted by Fe or other elements [5–6]. Co-free hydrogen storage alloy has got attention and there are some studies on it in recent years [7–8].

According to the pressure–temperature phase diagram, Co is known to exist in two allotropic forms: a low-temperature HCP phase and a high-temperature FCC phase [9–10]. However, bcc or more complex metastable structures have also been occasionally reported [11]. At room temperature, Co is stable in the HCP form but it transforms to the FCC form when it is heated to above the transition temperature 695 K. Because of its diffusionless character and the considerable thermal hysteresis between heating and cooling, this transformation is designated as martensitic [12]. Although allotropic HCP to FCC phase transformation via mechanical milling has been reported by several authors [13]. However, in spite of its apparent simplicity, the Co allotropic phase transition has not been fully understood yet.

The main purpose of this study is to determine for the first time an allotropic transformation of cobalt and a phase separation which occurs after melting and quenching alloys with different compositions of aluminium and cobalt in iron alloys.

2 Experimental materials and methods

The samples in this study were obtained by a high frequency induction fusion. Powder aluminium, iron and cobalt (99.999%) in proportions defined according to the composition aimed of alloy have been used. The total mass of the sample to be elaborated was between 8g and 10g. Cold compaction of mixed powder (Al-Fe-Co) under an uniaxial load of 10 MPa has been achieved to obtain a dense product (60%), which has been placed in a alumina crucible (Height: 3 cm, Diameter: 16 mm) introduced into a quartz tube and placed in the coil prior to high frequency fusion under primary vacuum (10^{-2} torr). Complete fusion of the alloys has been achieved at a temperature of about 1140°K. **Fig. 1a-b.**

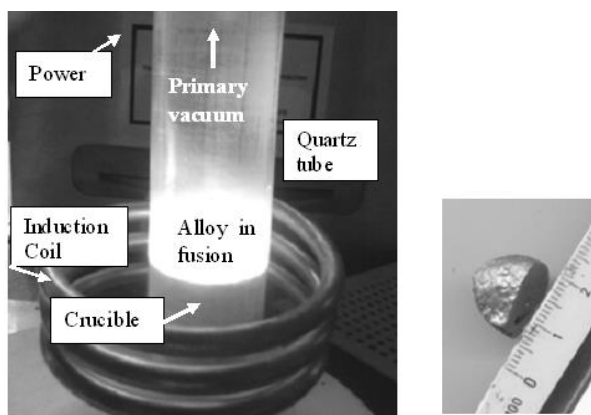


Fig. 1 (a) High frequency magnetic induction fusion system (b) shape and size of solidified Fe-Al-Co specimen

Light microscopy (Philips) has been used for structure observation. Differential scanning calorimetry DSC has been performed by Mettler Toledo Differential Scanning Calorimeter (with ADSC option) model DSC820 system STARe SW.9.20. The heating rate was about 20°mn^{-1} for a sample weight of 25mg. X-ray diffraction analysis has been performed by Philips X-ray diffractometer working with copper anticathode ($\lambda=0.154\text{nm}$) and covering 110° in 2θ .

3 Results and discussion

Addition of cobalt (5 at. %, 10 at. %, 15 at. % and 20 at. %) as a third element to binary Fe-40 % Al (Al-60% Fe) with ordered B_2 structure leads to important structural evolution, as shown by the ternary equilibrium phase diagram [14] **Fig. 2** and x- ray diffraction patterns of the Co containing alloys as well as light microscopy. **Fig. 3a-b-c-d-e** and **Fig. 4a-b.**

The broad halo which appears in the neighborhood of $2\theta = 16^{\circ}$ in B_2 ordered alloys and especially in the alloy containing 20%Co, is the result of chemical long range order [15]. We also note the presence of (100) superstructure reflexions at $2\theta = 30^{\circ}$. It follows that the grain size decreases with Co concentration between 5% and 15% and increases again until 20%Co. **Fig. 5** (fragmented x-ray diffraction pattern in the vicinity of (110) peak diffraction of B_2 phase showing the evolution of (110) peak half width with cobalt content addition. The B_2 -FeAl lattice constant variation is showed in **Fig. 6**. This evolution of the lattice parameter is not in line with

the decrease of the lattice parameter of other Fe based phases, where Co substitutes the Fe atom [16].

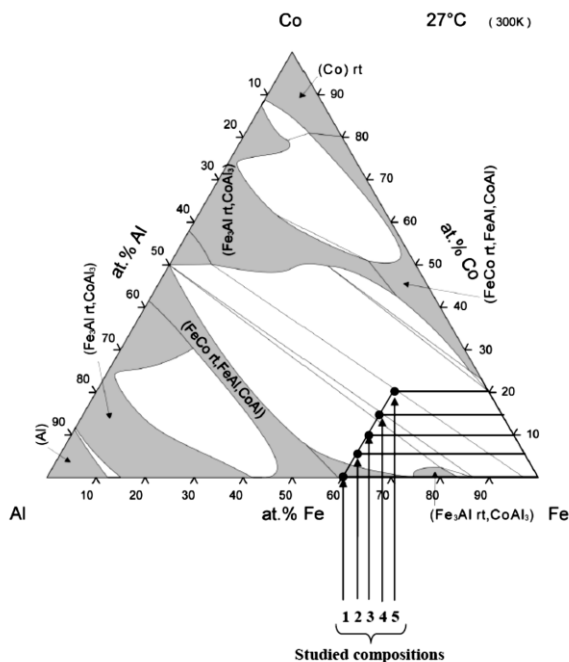


Fig. 2 Ternary Fe-Al-Co phase diagram at room temperature [14]. Compositions used in the present study are showed by arrows.

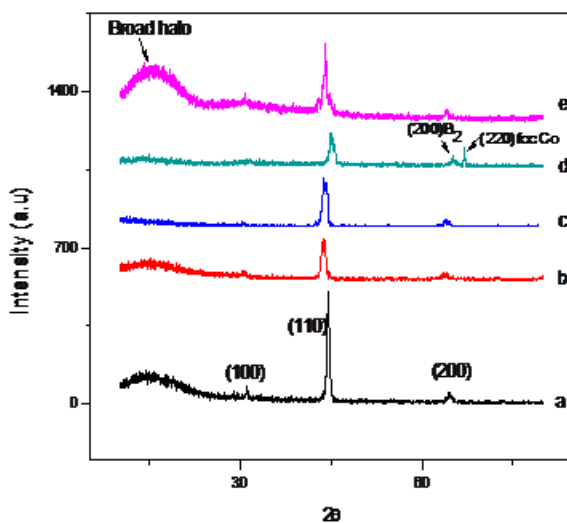


Fig. 3 X-ray diffraction pattern of various as-solidified Fe-Al-Co alloys, showing broad halos. 0 % Co, b) 5 % Co, c) 10 % Co, d) 15 % Co, e) 20 % Co

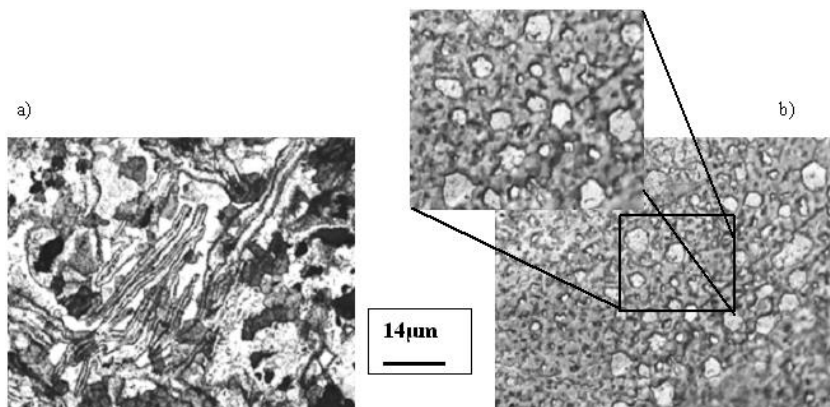


Fig. 4 Optical micrographs of Fe60%-Al35%-5%Co (a) and Fe60%-Al25%-15%Co (b) with dispersed cobalt.

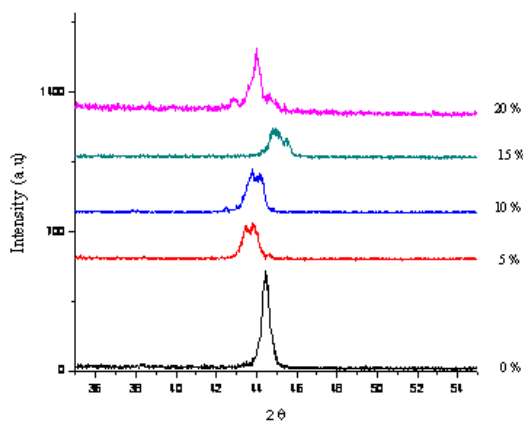


Fig. 5 Fragmented x-ray diffraction pattern in the vicinity of (110) peak diffraction showing phase separation

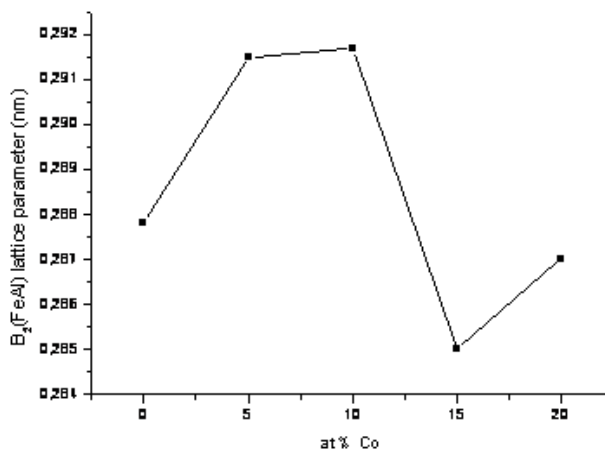


Fig. 6 $B_2(\text{FeAl})$ phase lattice constant variation versus Cobalt addition

Fig.4b shows hexagonal shaped Cobalt particles dispersed and embedded in B_2 -FeAl matrix with an average size of about $4\mu\text{m}$ and a volume fraction of about 30% (insert Fig.4b). X-ray diffraction pattern of **Fig. 3d** shows a sharp (220) FCC Cobalt Bragg peak beside (200) fundamental B_2 -FeAl reflexion located in the neighborhood of $2\theta = 68^\circ$. The inspection of the whole x-ray diffraction pattern reveals close packed hexagonal Bragg peaks of cobalt. With increasing Co concentration, the (110) diffraction peaks are shifted to lower angle and become broader than in free cobalt alloy. **Fig. 7a-c-d**, except for 20% Co (formation of quasi symmetric (110) side bands). **Fig. 7b**. The side bands take their origin from the cobalt allotropic transition from HCP to FCC, as revealed by (100) and (002) diffraction peaks. c/a ratio variation with cobalt addition is shown in Table1 and **Fig. 8**.

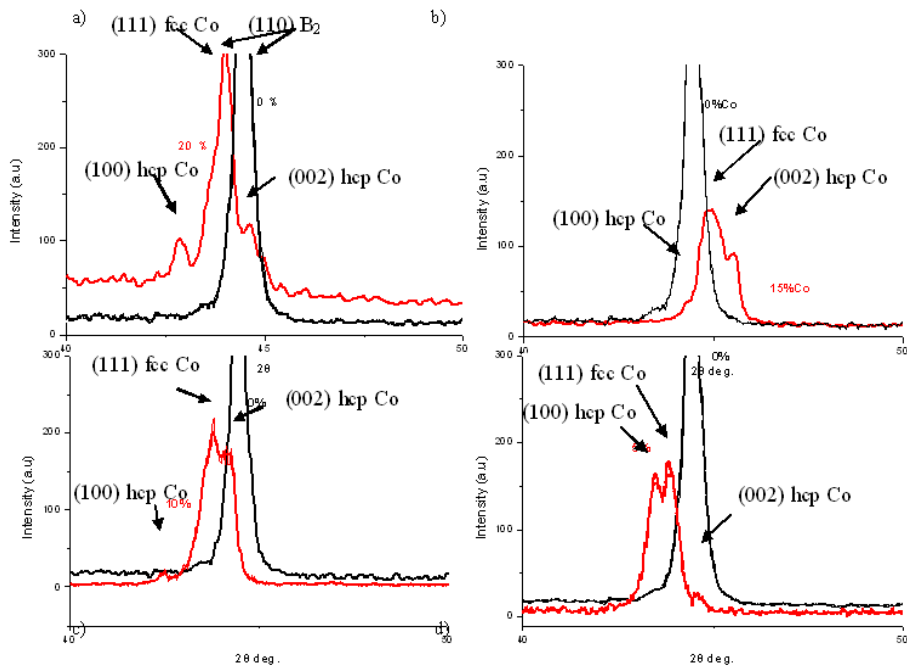


Fig. 7 Separation and shift of (110) Bragg peak with cobalt addition (Red line).

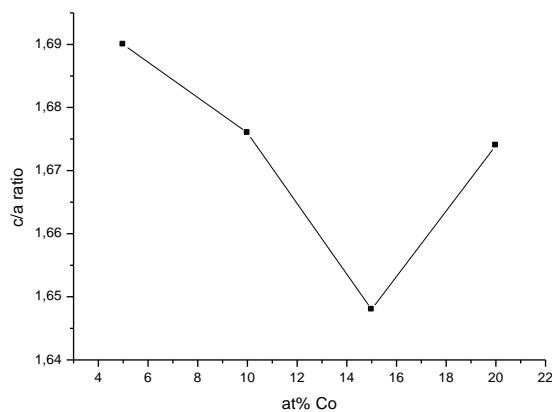


Fig. 8 HCP Cobalt lattice constants ratio (c/a) variation with cobalt content

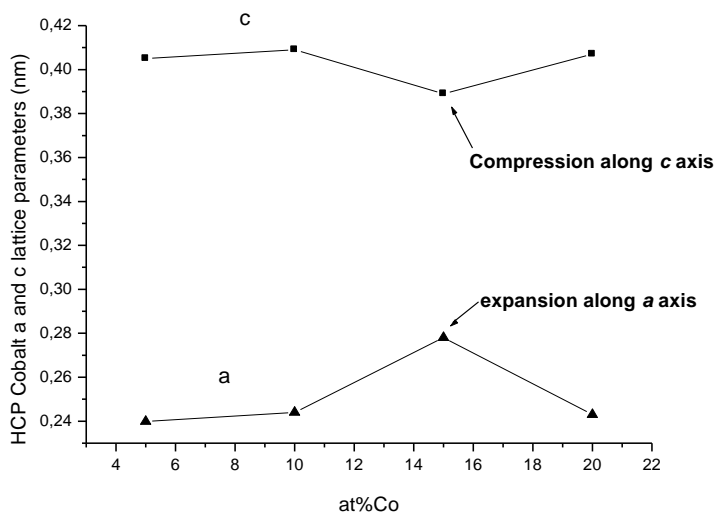


Fig. 9 (c) and (a) lattice parameters of HCP Cobalt variation with cobalt content.

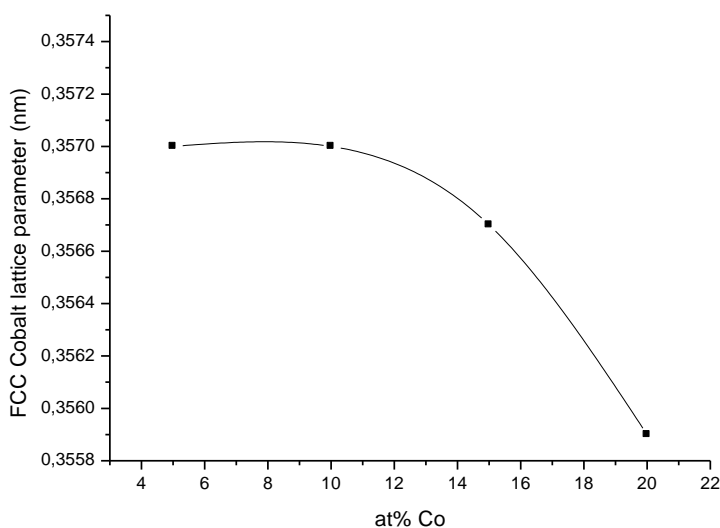
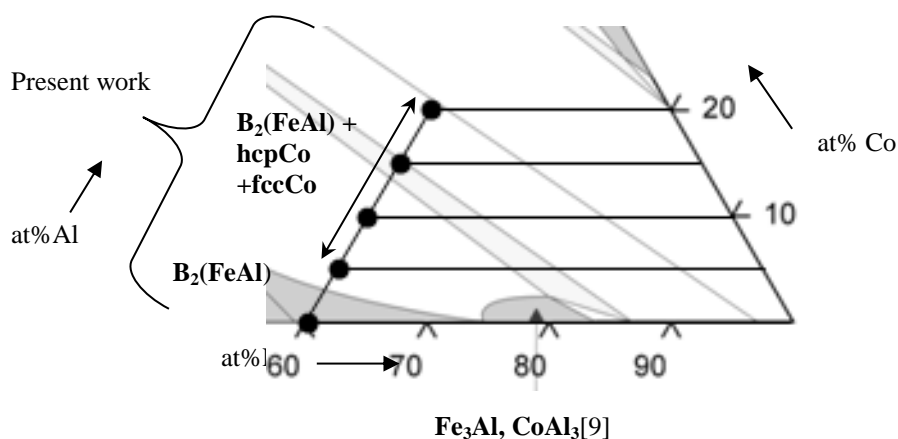


Fig. 10 Metastable FCC lattice parameter variation with cobalt content.

The lower value of c parameter is obtained at 15 % Co, it follows that the HCP crystal lattice was compressed more along the c -axis, as a consequence an expansion is obtained along a -axis ($a_{\text{HCP}} = 0.278$ nm) as shown by **Fig. 9** and **Table 1**, where values of a and c for hexagonal cobalt issued from JCPDS-ICDD [17] are reported. This effect looks like a martensitic transformation (from FCC to BCT) as described by Bain's model. **Fig. 10** shows the metastable FCC Cobalt lattice parameter variation with cobalt addition. The value obtained in the current work is around 0.357 nm, close to the previously reported value of 0.354 nm in mechanically milled Cobalt [18]. It follows that the grain size decreases with Co concentration between 5 % and 15 % and increases again until 20 %.

Table 1 Lattice parameter (nm) of allotropic forms from Cobalt in different alloys.

| Phase | | JCPDS-ICDD [17] | 5% | 10% | 15% | 20% |
|--------------|--------------------|--|-------|-------|-------|-------|
| Cobalt (HCP) | Lattice parameters | a= 0.251 c = 0.407 | 0.239 | 0.244 | 0.278 | 0.243 |
| | | P6 ₃ /mmc JCPDS-ICDD (41-1487) | 0.405 | 0.409 | 0.389 | 0.407 |
| | <i>c/a</i> | 1.621 | 1.690 | 1.676 | 1.648 | 1.674 |

**Fig. 11** Portion of the ternary phase diagram showing the phase separation.**Table 2** Structural evolution of various Fe-Al-Co alloys in relation with alloying element composition.

| Composition (Cobalt) | 0% (1) | 5% (2) | 10% (3) | 15% (4) | 20% (5) |
|----------------------|-----------------------|---------------------------------------|---------------------------------------|---------------------------------------|---------------------------------------|
| Structure | B ₂ (FeAl) | B ₂ (FeAl) + hcpCo + fccCo | B ₂ (FeAl) + hcpCo + fccCo | B ₂ (FeAl) + hcpCo + fccCo | B ₂ (FeAl) + hcpCo + fccCo |

Cobalt addition as third element to binary Al-60 % Fe leads to a phase separation of B₂-FeAl, **Table 2** and **Fig. 11**. As a consequence, the hardness decreases until 10 % Co (critical composition) and then exhibits an increase until 15 % Co followed by a slow evolution in the vicinity of 20 % Co, **Fig. 12**. This makes cobalt addition more advantageous in regard to iron addition since the detrimental effect of iron on ductility is due to the size and number density of iron-containing intermetallics, the more intermetallics there are, the lower the ductility [19-20-21].

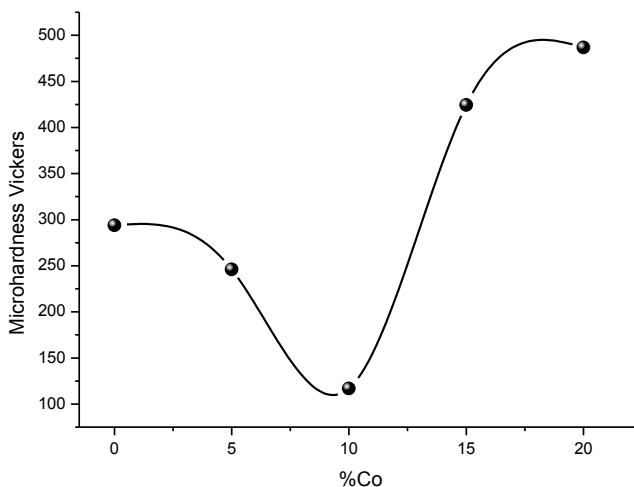


Fig. 12 B_2 (FeAl) Microhardness variation with Cobalt addition.

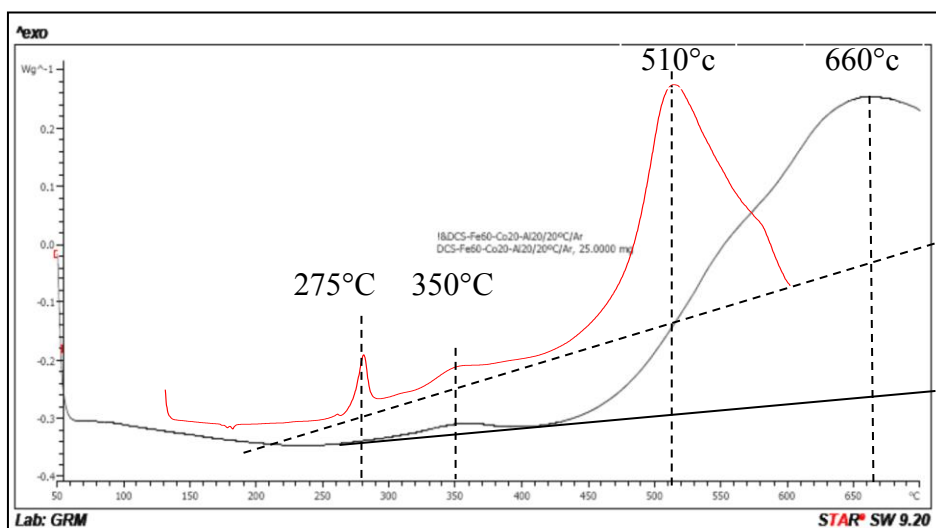


Fig. 13 DSC superposition of both binary Al-60 % Fe (Red line) and ternary Al-60 % Fe-20 % Co.

As a comparative perspective between the free cobalt alloy Fe-40%Al (Al-60 % Fe) DSC curve (red line), and Al-60 % Fe-20 % Co (black curve) **Fig. 13**, the alloys were submitted to a differential scanning calorimetry (DSC) study without annealing. The DSC curve monitored from binary Fe-40 % Al shows three different exothermic peaks at around $T_1 = 200^\circ\text{C}$; $T_2 = 300^\circ\text{C}$ and $T_3 = 500^\circ\text{C}$. Thus, the first transformation ($T_1 = 200^\circ\text{C}$), only detected in this as-cast alloy, may be associated with the ordering process to the B_2 phase. A further increase in the measuring temperature seems to give rise to the final partial ordering process from B_2 to DO_3 superstructure (detected as a small hump around 300°C in the DSC curve. Finally, the transformation peak around 500°C should be ascribed to a recovery process (i.e. relaxation of

high-temperature quenched-in defects). DSC curve monitored from ternary Fe-40 % Al-20 % Co shows abroad exothermic peak at 660°C and may be the result of the allotropic transformation from HCP to FCC Cobalt that occurs in this alloy as shown in **Fig.7a** by shift of (110) Bragg peak and apparition of side bands. The less important DSC peak at 350°C is due to ordering process from B₂ to DO₃ superstructure.

4 Conclusion

As we can gather from our discussion, the main results of the present study are: A drastic and significant structural changes occur by addition of cobalt between 5% and 20% to binary B₂ ordered Fe-Al alloys system produced by high frequency induction fusion, as revealed by DSC analysis and x-ray diffraction. A phase separation of both HCP and FCC Cobalt which may be a contribution to the enhancement of ternary phase diagram, is highlighted for the first time in all studied ternary Fe-Al-Co elaborated by high frequency induction fusion prior to solidification at room temperature.

References

- [1] H. Xiao, I. Backer: *Acta Metallurgica et Materialia*, Vol. 43, 1995, No. 1, p. 391-396
- [2] J. N. Barbier., N.Tamura, J.-L Verger-Gaugry: *Journal of Non Crystalline Solids*, Vol. 153, 1993, No. 172, p. 126-131
- [3] W. Feng, Z. Min-Yu, M. Dao-Bin: *Transactions of NonFerrous Metals Society of China*, Vol. 20, 2010, No. 10, p. 1885-1891
- [4] L. Yi-Xin et al.: *Journal of Hydrogen Energy*, Vol. 34, 2009, No. 7, p. 2986-2991, DOI: 10.1016/j.ijhydene.2008.08.052
- [5] Z. Yanghuan, et al.: *Rare Metal Materials and Engineering*, Vol. 35, 2006, No. 2, p. 277-282
- [6] C. Li-Fang et al.: *Rare Metal Materials and Engineering*, Vol. 35, 2009, No. 3, p.451-455
- [7] W. Xuedong et al.: *Journal of Alloys and Compounds*, Vol. 458, 2008, No. 8, p. 583-587, DOI: 10.1016/j.jallcom.2007.04.211
- [8] H. Shao et al.: *Journal of Alloys and Compounds*, Vol. 479, 2009, No. 9, p. 409-413, DOI: 10.1016/j.jallcom.2008.12.067
- [9] J. Sort, J. Nogue, S. Surin, M. D. Baro: *Philosophical Magazine*, Vol. 83, 2003, No. 4, p. 439-455, DOI: 10.1080/0141861021000047159
- [10] S. Sun, C.B. Murray: *Journal of applied Physics*, Vol. 85, 1999, No. 8, p.4325-4331, DOI: 10.1063/1.370357
- [11] S. Kajiwara, S. Ohno, K.Honma: *Philosophical Magazine*, Vol. 63, 1991, No. 4, p. 625-644, DOI: 10.1080/01418619108213904
- [12] T.Krenke et al.: *Physical Review B*, Vol. 72, 2005, No. 1, 014412-01442, DOI:10.1103/PhysRevB.72.014412
- [13] J. Y. Huang et al.: *Nanostructured Materials*, Vol. 6, 1995, No. 5-8, p. 723-726, DOI: 10.1016/0965-9773(95)00160-3
- [14] D. A Young: *Phase Diagrams of the Elements*, University of California Press, Berkeley, California, 1991
- [15] T. Schenk et al.: *Europhysics Letters*, Vol 65, 2004, No. 1, p. 34-40, DOI: 10.1209/epl/i2003-10062-x

- [16] F. Delogu: *Scripta Materialia*, Vol 58, 2008, No. 2, p. 126–129, DOI: 10.1016/j.scriptamat.2007.09.021
- [17] T. G. Fawcett et al.: *Microstructure Analysis in Materials Science*, Freiberg, June 15 – 17, 2005
- [18] S.G.E.Velthuis et al.: *Acta Materialia*, Vol. 46, 1998, No. 15, p. 5223-5228, DOI: 10.1016/S1359-6454(98)00248-1
- [19] A. Couture: *AFS International Cast Metals Journal*, Vol. 6, 1981, No. 4, p. 9-17
- [20] P. N. Crepau: *AFS Transactions*, Vol. 103, 1995, p. 361-366
- [21] T.O. Mbuya et al.: *International Journal of Cast Metals Research*, Vol. 16, 2003, No.5, p. 451-465